HiSST: 3rd International Conference on
High-Speed Vehicle Science Technology
14 -19 April 2024, Busan, Korea

Flyability Assessment and Trajectory Design for a Scramjet Hypersonic Experimental Vehicle

A. Vitale[1], S. Di Benedetto[1], M. Marini[1], S. Pizzurro[2], R. Bertacin[2]

Abstract

Flying faster and higher to reduce travel times on long haul routes is one of the main goals of the aerospace research in the last decades. Flight mechanics analyses play a critical role in the development of high-speed vehicles, from their conceptual design till to the flight test execution and post flight studies aimed at the exploitation of experimental data. This paper describes the flight mechanics activities performed in the preliminary design phase of a hypersonic demonstrator, which is based on the waverider concept and equipped with a scramjet air-breathing propulsion system. Its experimental mission envisages an air-launched solution and exploits a launch vehicle to achieve the desired experimental conditions. Specifically, the paper presents and discuss the analyses executed to investigate the hypersonic demonstrator's flyability properties and to define the mission nominal trajectory. The former analyses exploit the aerodynamic database to assess trimmability, manoeuvrability and static stability of the vehicle on the whole flight envelope of interest. Trajectory computation is carried out by solving a constrained nonlinear optimization problem, which takes into account the compliance to the applicable mission requirements and system constraints. Obtained results provide useful information concerning the optimal vehicle configuration and confirm the feasibility of the flight test.

Keywords: *high speed, hypersonic vehicle, flight mechanics, trajectory optimization, flyability analyses*

Nomenclature

Latin
ADB – Aerodynamic DataBase
C_D – Drag nondimensional coefficient
C_L – Lift nondimensional coefficient
C_m – Pitching moment nondimensional coefficient
CoG – Centre of Gravity
aerodynamic coefficient
G_{man} – Maneuverability margin
h – Altitude
J – Objective function
M – Mach number
MCI – Mass, Centring, Inertia
RMS – Root Mean Square
SM – Static Margin
t – Time
x – State vector of the vehicle

Greek
α – Angle of attack
δ – Flap deflection

Subscripts
α – Derivative with respect to angle of attack

1. Introduction

Flying faster and higher to reduce travel times on long haul routes is one of the main goals of the aerospace research in the last decades. The Italian Aerospace Research Centre (CIRA) has been strongly engaged on this research topic for twenty years, having been part of several European and

[1] *Italian Aerospace Research Centre (CIRA), Via Maiorise 81043, Capua (CE), Italy, a.vitale@cira.it, s.dibenedetto@cira.it, m.marini@cira.it*
[2] *ASI, Agenzia Spaziale Italiana, 00133 Rome, Italy, simone.pizzurro@asi.it, roberto.bertacin@asi.it*

national projects concerning hypersonic flight for passenger transport and military applications. The latest one "SPACE-IPERSONICA-TEC", funded by the national program on aerospace research PRORA and coordinated by CIRA, fits perfectly into this research framework, with the objective to increase the technology readiness level of the key technologies for future hypersonic transport vehicles. The high interest also of the Italian Space Agency in the field of hypersonic flight led the two national entities to co-fund the research activities by a dedicated agreement "Research and Development of a hypersonic demonstrator", which main objective is the design of a propelled hypersonic demonstrator that is able to perform level and controlled flight at Mach 6÷8 and at altitudes of 27÷32 km, with the aim to develop and test in flight the enabling technologies for the implementation of the future transportation systems at hypersonic speed [1]. The two projects will be referred in the following as project.

Flight mechanics play a fundamental role in the development of such a demonstrator, from the conceptual design of the vehicle and its planned mission, till to the execution of the flight test and the post flight studies aimed at the exploitation of the data collected during the experimental mission. In fact, during the design and development of a new vehicle, flight mechanics allow the evaluation of the vehicle's flying qualities and the optimization of the mission profile [3]. These analyses permit to assess the compliance to mission and system requirements and provide guidelines to the designers concerning the optimization of aircraft aerodynamic and inertial configuration. Moreover, they compute the allowable ranges of variation (or uncertainties) for some critical vehicle parameters [4], such as the centre of gravity position and the aerodynamic derivatives, which on one side define for the planned mission the sizing conditions and on the other side are inputs for the design and numerical validation of critical subsystems, such as guidance navigation and control, propulsion, and thermal protection systems. In addition, before flight, flight mechanics simulation models can be exploited to support safety assessment. Finally, after the execution of the flight test, flight mechanics analyses use experimental data to perform system identification aimed to improve the comprehension of the vehicle characteristics and to refine the models that represent its dynamics [5].

This paper describes the flight mechanics analyses performed in the preliminary design phase of the project, concerning the assessment of the vehicle's flyability properties and the definition of the nominal trajectory, with the aim to provide guidelines on the demonstrator configuration and to assess the feasibility of the flight mission. Next sections of the paper first describe the demonstrator concept and planned mission (section 2), next presents the performed analyses objectives and methodologies (section 3), and then discuss the obtained results (section 4). Finally, a conclusions section ends the paper.

2. Hypersonic Flight Demonstrator and Experimental Mission Concept

The Scramjet Hypersonic Experimental Vehicle (SHEV), which is the demonstrator under development in the framework of the project, is shown in Fig.1. It is based on the concept of "waverider", that is, a hypersonic vehicle with high aerodynamic efficiency obtained through the exploitation of the shock waves that form on the load-bearing surfaces. The demonstrator includes a scramjet air-breathing propulsion system.

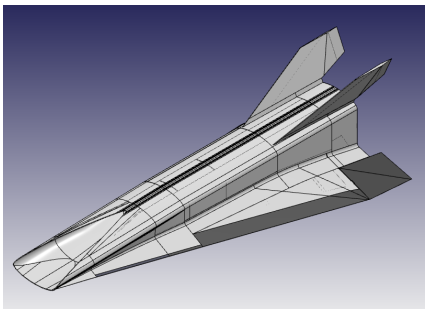

Fig 1. Scramjet Hypersonic Experimental Vehicle

The preliminary mission concept is shown in Fig.2 [2]. It envisages an air-launched solution with a carrier capable of releasing the payload at a target point (sep1), defined in terms of speed and altitude. The payload is composed of the propelled hypersonic demonstrator and a launch vehicle equipped with a booster. After sep1, the booster accelerates until it reaches the experimental window (target altitude and Mach) and releases the hypersonic demonstrator (sep2). Next, the scramjet on board the

demonstrator turns on and operates for at least 10 seconds; the demonstrator shall perform a hypersonic flight at constant altitude, guaranteeing a positive aero-propulsive balance and aerodynamic efficiency in the range 3÷4. Finally, the scramjet shuts off, and the demonstrator glides decelerating until the vehicle becomes uncontrollable and splashes down.

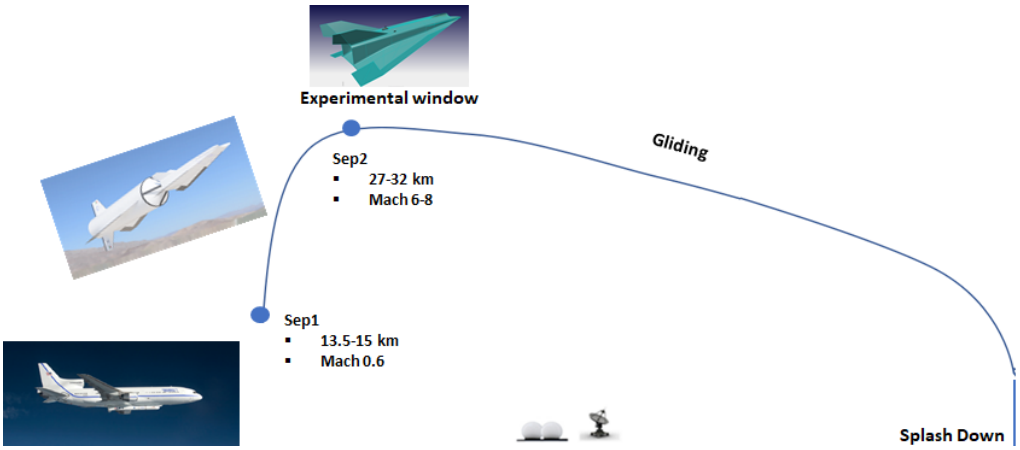

Fig 2. SHEV Mission concept

The flight mechanics analyses presented in this paper focus on the mission phase after sep2, which is composed by two legs: the experimental window and the gliding leg. Moreover, the mission is assumed purely longitudinal, therefore all the analyses are limited to the longitudinal dynamics.

3. Flight Mechanics Analyses Definition

3.1. Analyses Objectives

The flight mechanics analyses aim at evaluating the SHEV flyability properties on the whole envelope where the aerodynamic data are available, and at defining the nominal trajectory that fits the desired experimental mission profile. The completion of both these tasks allows to check the feasibility of the mission and to compute the optimal position of the demonstrator's centre of gravity (CoG), supporting the definition of the vehicle configuration. Fig.3 presents the flowchart of these analyses and the required inputs.

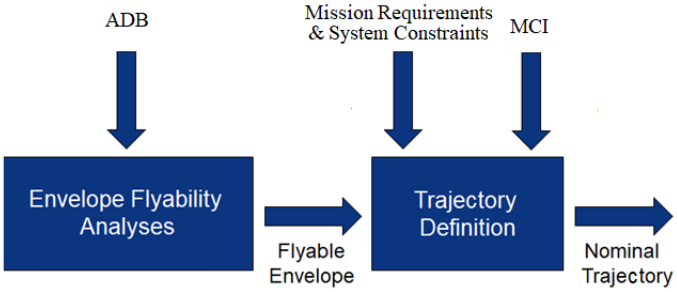

Fig 3. Flight mechanics analyses activity flow

3.2. Analyses Methodologies

For a mission that is assumed purely longitudinal, the flyability analyses assess, in each point of the Mach number (M) – angle of attack (α) plane, the vehicle capability to achieve rotational trim in the longitudinal plane, to manoeuvre and to be static stable in the trim points, that is, to satisfy the following properties:

$$\exists \delta_{Trim} \in [\delta_{min}, \delta_{max}] \; such \; that \; C_m(M, \alpha, \delta_{Trim}) = 0 \tag{1}$$

$$(1 - G_{man}) \cdot \delta_{min} \leq \delta_{Trim} \leq (1 - G_{man}) \cdot \delta_{max} \tag{2}$$

$$C_{m\alpha}(M, \alpha, \delta_{Trim}) < 0 \tag{3}$$

$$SM = -(C_{m\alpha}(M, \alpha, \delta_{Trim}) / C_{L\alpha}(M, \alpha, \delta_{Trim})) > 0 \tag{4}$$

where δ_{min} and δ_{max} indicate the minimum and maximum allowable deflection of the flap, respectively, which usually have opposite sign; G_{man} is the manoeuvrability margin, which varies between 0 and 1 (it is usually about 0.2).

Eq. 1 formalizes the trim property, which consists in the capability to make null the pitching moment coefficient by deflecting the flap within its allowable envelope. The manoeuvrability property, expressed by Eq. 2, requires that the trim is obtained by using only a fraction of the available flap deflection, leaving the residual deflection, quantified by the manoeuvrability margin, to manoeuvre the vehicle around the trim condition. Finally, Eq. 3 and Eq. 4 define the static stability in the trim point, that expresses the ability of the vehicle to produce a variation of the pitching moment coefficient that opposes to a perturbation of the angle of attack, tending to restore the initial trim condition. The static margin in Eq. 4 provides the distance between the centre of gravity actual position and the neutral point (that is, the point in which the CoG shall be positioned to make the vehicle statically neutrally stable); therefore, when it is positive, it indicates how much (in terms of percentage of the aerodynamic reference length) the CoG could be shifted rearward while keeping the static stability. It is worthy to remark that these properties depend on the position of the vehicle centre of gravity, and usually trim and static stability have conflicting requirements on the CoG placement, as schematically shown in Fig.4. For this reason, a sensitivity analysis of the flying qualities is carried out, in order to identify the region in which the CoG can be placed keeping good flyability characteristics.

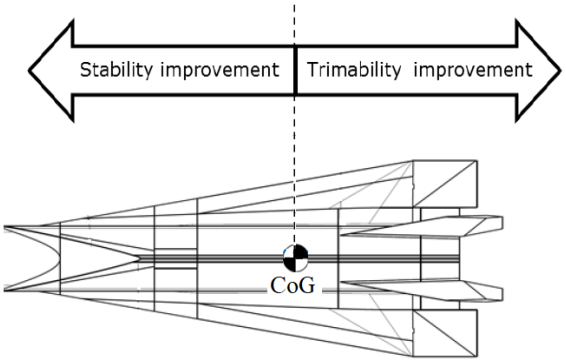

Fig 4. Effect of the centre of gravity location variation on trim and static stability

The definition of the nominal trajectory consists in computing the guidance law of the vehicle, which for a longitudinal mission coincides with the angle of attack profile. Next, this profile is used to obtain the vehicle position and velocity time history (and the time histories of all the parameters that are relevant for mission analysis, such as load factors and heat flux), by applying the flight mechanics longitudinal translational equations of motion [6] in which the angle of attack is the only input.

The computation of the guidance law requires the solution of the following nonlinear constrained optimization problem:

$$\min_{\alpha} J \quad such\ that \quad \begin{cases} \dot{x}(t) = F(\alpha(t), x(t), t) \\ B(\alpha(t), x(t), t) = 0 \\ C(\alpha(t), x(t), t) \leq 0 \\ \alpha_{min}(M) \leq \alpha(M) \leq \alpha_{max}(M) \end{cases} \tag{4}$$

The objective function J has to be properly selected and several choices are possible. The proposed approach consists in computing a reference profile in the Mach-altitude plane which translates the mission concept of Fig. 2 and is obtained by suitably scaling the X-43A mission [7]. Then, J is defined as summation of two terms: the RMS error with respect to the reference profile in the Mach-altitude plane, and the variation of the angle of attack at Mach number lower than 3. Indeed, at low Mach number the altitude profile with respect to Mach is poorly sensitive to the angle of attack; the introduction of the second term in the J function allows minimizing the manoeuvres in the final part of the mission and reducing the dependency of the obtained guidance law from the initial guess for angle of attack profile, which is required to solve the constrained optimization problem. Concerning the optimization constraints:

- the first equation represents the vehicle's translational dynamics, in which the vehicle is considered as a three degrees of freedom point mass, with constant mass and in trimmed aerodynamic conditions, moving around a spherical rotating Earth within a standard atmosphere in stationary (null winds) state;
- the equality constraint defines the nominal trajectory initial and final points;
- the first inequality derives from the mission requirements and system constraints applicable to nominal trajectory design;
- the second inequality identifies the admissible range of variation for the angle of attack that guarantees good flyability properties.

The resolution of the optimization problem formalized by Eq. 4 can be simplified using some engineering considerations:

- the two mission legs (experimental window and gliding) are analysed independently;
- in the first leg (experimental window), the angle of attack is assumed constant and equal to the value (if it exists) that guarantees constant altitude, aerodynamic efficiency bigger than 3 and positive aero-propulsive balance, as requested by mission concept;
- in the second the leg (gliding phase), the angle of attack profile is defined through nodal points with respect to Mach number values, which decrease monotonically in this leg; the variation of α between two nodal points is assumed linear.

In the first leg, the angle of attack is selected within the range in which the aerodynamic efficiency is bigger than 3 and the aero-propulsive balance is positive, and selected as the value that produces an aerodynamic force able to balance the weight of the vehicle, thus guaranteeing the vertical equilibrium. In the second leg, the computation of the angle of attack values in the nodal points is carried out numerically, by using the Matlab minimization routine "fmincon" [8] and an active-set strategy [9]; null values are assumed as initial guess. No condition is imposed on the angle of attack transition between first leg and second leg, except for an a posteriori check that the variation of the angle in the transition is lower than 1 degree (during actual flight, this discontinuity will be smoothed by the vehicle dynamics).

4. Flight Mechanics Analyses Results

4.1. Input Data

Three types of external inputs are required to perform the flight mechanics analyses, as sketched in Fig. 3: aerodynamic database, inertial data (mass and centring), mission requirements and preliminary system constraints.

The aerodynamic database provides the longitudinal nondimensional aerodynamic coefficients (that is, lift, drag and pitching moment) for both motor-on and motor-off conditions. Each coefficient is composed of two additive terms: a clean contribution, which assumes null flap deflection, and a flap contribution. When the motor is on, the aerodynamic clean contribution includes also the generated thrust force, thus the net force could accelerate the vehicle (that is, the drag could become negative). All the contributions refer to the centre of gravity as aerodynamic pole; they are defined on the envelopes listed in table 1.

Table 1. Definition envelope of the aerodynamic coefficients

Aerodynamic contribution	Mach number range	Angle of attack range [deg]	Flap deflection range [deg]
Clean motor-on	7.35	-2 ÷ 2	0
Clean motor-off	2 ÷ 7.35	-2 ÷ 4	0
Flap	2 ÷ 7.35	-2 ÷ 4	-20 ÷ 10

Fig. 5 and Fig. 6 show the clean contribution to the aerodynamic coefficients for motor-on and motor-off, respectively. Fig. 7 presents the flap contribution to the lift coefficient, which is the most interesting one; indeed, it highlights that, at low Mach number and for negative flap deflection (typically required

to trim hypersonic vehicle) bigger than 10 degrees, the contribution to lift is negative and not negligible with respect to the clean coefficient. In this case, the flap produces a significant reduction of the global lift coefficient.

It is worthy to remark that the trimmed aerodynamic database is required for the computation of the nominal trajectory. The trimmed ADB has coefficients depending only on Mach number and angle of attack, because the flap deflection is set equal to the value that guarantees the rotational trim for each couple (M, α). Since the trim depends on the CoG position, then the centre of gravity location affects also the trimmed ADB and therefore the computation of the nominal trajectory.

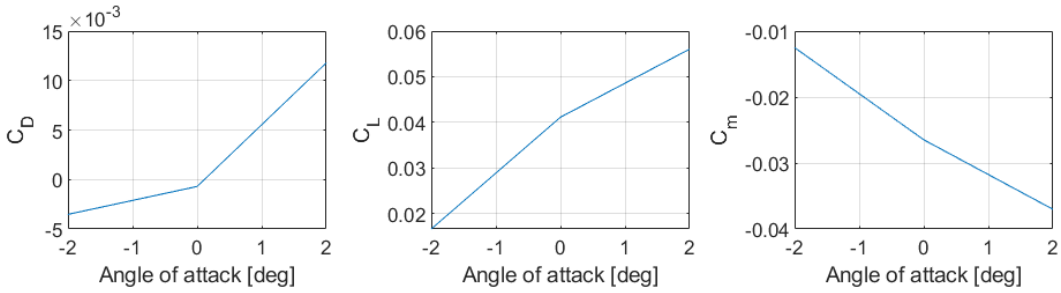

Fig 5. Clean contribution to nondimensional aerodynamic coefficients for motor-on

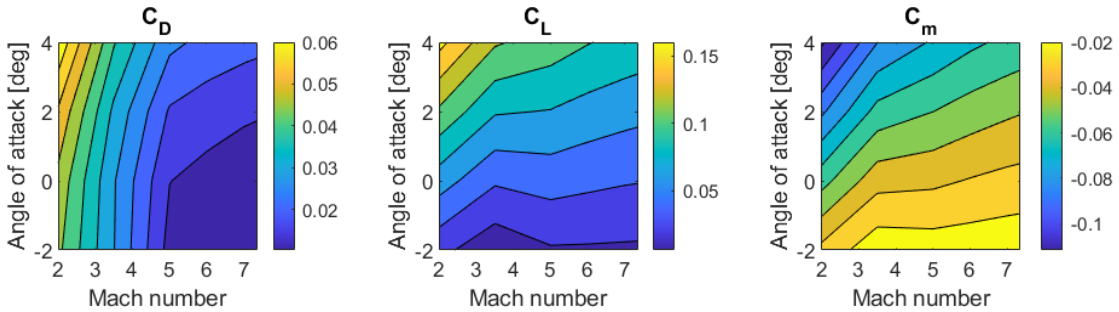

Fig 6. Clean contribution to nondimensional aerodynamic coefficients for motor-off

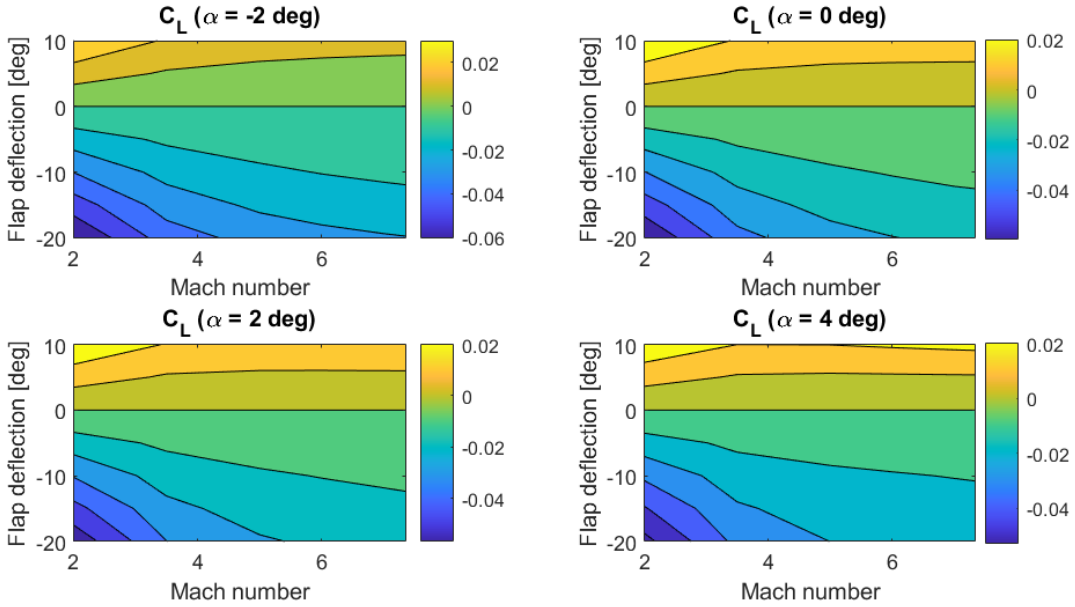

Fig 7. Flap contribution to lift nondimensional coefficient for different values of the angle of attack

For what concerns the inertial data, only two parameters are required: the nominal mass, which is 1120 Kg, and the nominal position of the centre of gravity, which is located on the longitudinal axis of the vehicle at 2326.4 millimetres from the nose (the reference length of the demonstrator is 4124,8 millimetres, that is, the CoG is located at 56.4% of the reference length).

Preliminary mission requirements and system constraints (to be confirmed in the following project phases) are presented in table 2 and table 3, respectively. In compliance with requirement R1, it is assumed that the experimental window nominally starts when the vehicle is at 27 km altitude and its speed is 2203 m/s, corresponding to Mach 7.35.

Table 2. Mission requirements

Identifier	Requirement
R1	The demonstrator shall perform a hypersonic flight at Mach = 6÷8 and constant altitude = 27÷32 km
R2	The demonstrator with motor on shall have a positive aero-propulsive balance with aerodynamic efficiency L/D=3÷4 at Mach 6÷8
R3	The scramjet propulsion system shall work and be stable for at least 10 seconds
R4	The demonstrator shall be trimmable and controllable along the whole trajectory

Table 3. System constraints (preliminary)

Identifier	Constraint
C1	Maximum dynamic pressure: 72 kPa
C2	Maximum acceleration: 3g
C3	Maximum heat flux: 635 kW/m^2
C4	Maximum heat load: 97.62 MJ/m^2

4.2. Flyability Analyses

The flyability analyses have been executed for different positions of the centre of gravity along the vehicle's longitudinal axis (keeping constant the coordinates along Y and Z axes), in order to carry out a sensitivity analysis of the vehicle performance. The considered CoG are located at a distance between 2161.4 millimetres and 2491.4 millimetres from the vehicle's nose, with the initial nominal CoG placed at 2326.4 millimetres, exactly in the middle of the examined range. The analyses result pointed out that satisfactory flyability properties are guaranteed if the centre of gravity position is between 2243.9 and 2309.9 millimetres.

Flyability properties for the CoG placed at the forward limit of the identified range are shown in Fig. 8. If the motor is turned off, the vehicle is trimmable almost everywhere, except for a small region at angle of attack bigger than 3 degrees and Mach number between 3 and 4.5; the flap deflection required to trim is always negative, as expected for this type of vehicle. The manoeuvrability margin is always bigger than 20%, when the angle of attack is lower than 3 degrees, except for a small region around Mach 3 where it slightly reduces, remaining however always bigger than 10%. The static stability is guaranteed in the whole trimmable region. If the motor is on, the vehicle is always trimmable and static stable. A manoeuvrability margin bigger than 20% is available for angle of attack lower than 1 degree; it reduces to 5% for angle of attack equal to 2 degrees. The static margin is bigger than 3% for negative angle of attack, whereas it increases to about 15% for positive values of angle of attack. If the angle of attack is bigger than -0.55 degrees, then the aerodynamic efficiency is bigger than 3, guaranteeing the compliance with mission requirement R2. It is worthy to highlight that moving the CoG forward with respect to the considered position produces an enlargement of the region where the vehicle is not trimmable and a reduction of the manoeuvrability margin, which could have an impact on the trajectory feasibility especially for motor off, in addition to a significant displacement with respect to the original CoG nominal position, which needs an assessment at system level. For these reasons the forward CoG limit from the flyability analyses perspective is set at 2243.9 millimetres.

Fig. 8, as well as the following Fig. 9, shows the nominal trajectory (the computation of which is discussed in the next section) in addition to the flyability properties. When the motor is off, the trajectory is represented as a broken line in the Mach number - angle of attack plan, to be tracked

during the whole decelerating gliding phase. Instead, when the motor is on, it is just a point that identifies the angle of attach to be kept at Mach = 7.35 during the experimental window.

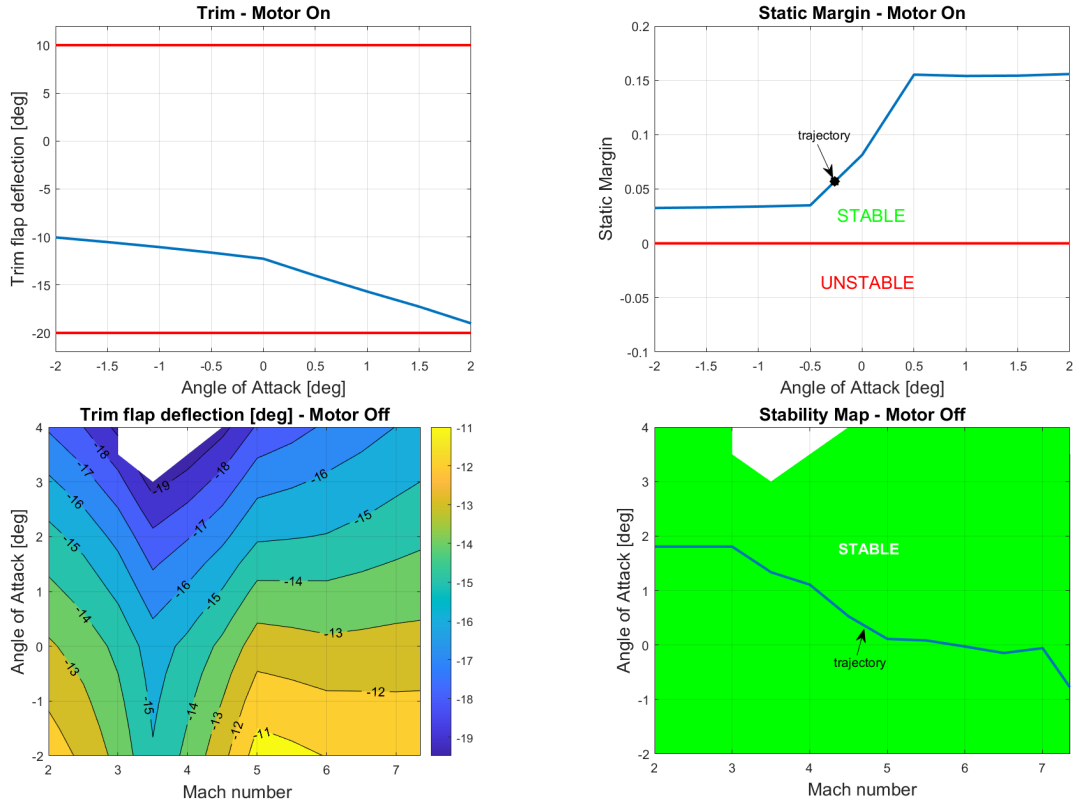

Fig 8. Flyability properties for centre of gravity at 2243.9 mm from the vehicle nose and nominal trajectory plotted on the stability map

Fig. 9 presents the flyability properties for the CoG placed at the rearward limit of the identified allowable range. The vehicle is trimmable and manoeuvrable on the whole examined flight envelope, that is, for Mach between 2 and 7.35 and angle of attack between -2 and 4 degrees when the motor is off, and for Mach equal to 7.35 and angle of attack between -2 and 2 degrees when the motor is on. Also in this case, the flap deflection required to trim is negative, that is, the clean vehicle tends to pitch down. The manoeuvrability margin is always higher than 20%, except for Mach close to 3.5 where it reduces to 15%. If the motor is turned off, then there is a wide stability corridor in which the trajectory can be placed, as shown in the figure. The stability margin, shown for motor on, values few percentage points if the angle of attack is negative, as typical for hypersonic vehicle; for positive angle of attack, it increases above 10%. If the angle of attack is bigger than -0.7 degrees, then the aerodynamic efficiency is bigger than 3, guaranteeing the compliance with mission requirement R2. It is worthy to point out that the shift of the CoG rearward with respect to the considered position enlarges the instability region, constraining the trajectory to cross it; although the instability characteristics shall be further investigated in terms of dynamics behaviour and could be mitigated by introducing a stability augmentation system, the obtained results suggest to set as rearward limit for the CoG the position at 2309.9 millimetres.

Based on these results, the identified CoG range is only long 66 millimetres, that is, 1.6% of aerodynamic reference length (from 54.4% to 56%), requiring high accuracy and precision in locating the CoG, which shall be place slightly forward with respect to the initially selected nominal position.

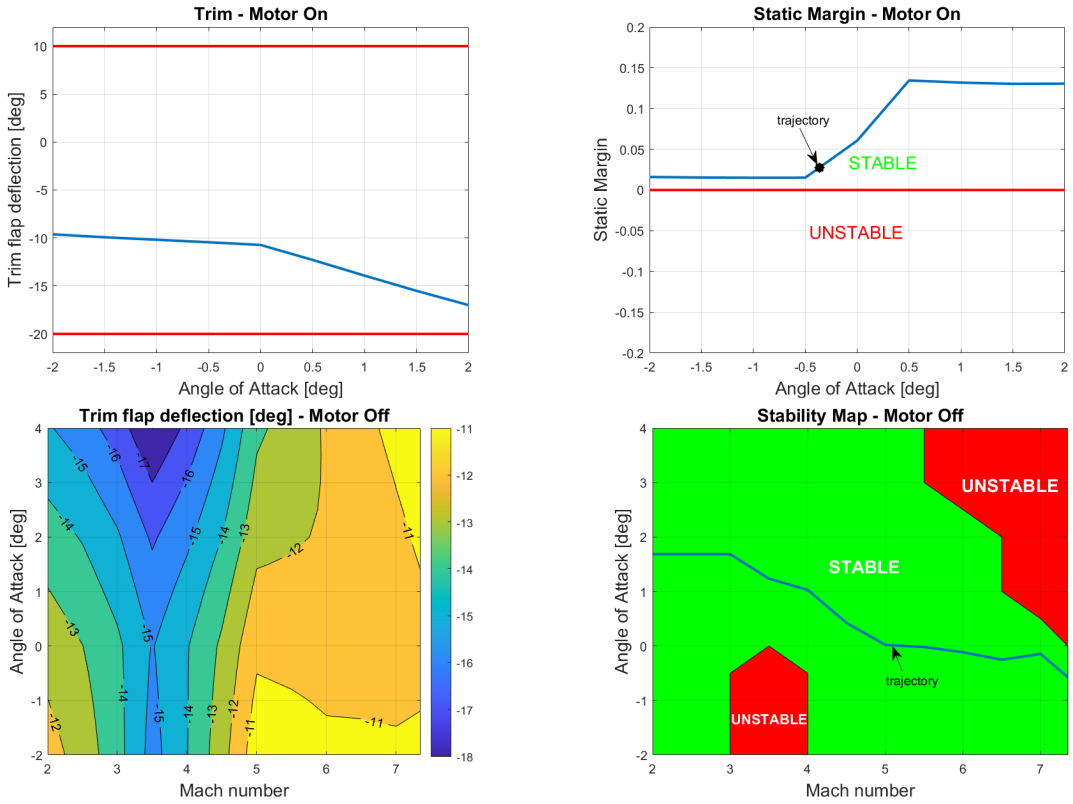

Fig 9. Flyability properties for centre of gravity at 2309.9 mm from the vehicle nose and nominal trajectory plotted on the stability map

4.3. Nominal Trajectory

Nominal trajectory has been computed for different positions of the centre of gravity belonging to the range that guarantees good flyability properties. Fig. 10 to Fig. 12 present the results for the CoG placed at the limits of this range (that is, CoG at 2243.9 millimetres and 2309.9 millimetres from the vehicle nose). For centre of gravity in intermediate positions the analyses provide similar results, which are not discussed here for the sake of brevity.

The computed nominal trajectories are always within the static stability region (see Fig. 8 and Fig. 9); the experimental window, when the motor is on, lasts 10 seconds at constant altitude and Mach equal to about 7.35. In this flight condition, the aerodynamic efficiency is bigger than 3 and the aero-propulsive balance is positive (that is, the thrust is bigger than the drag).

Fig. 10 shows the nominal trajectory in the Mach-altitude plane for the two CoG positions, and compares them with the reference profile that implements the mission concept: the nominal trajectories are in practice undistinguishable from the reference one. Time histories of Mach number and altitude are presented in the same figure. After the experimental window, both the variables decrease smoothly decelerating the vehicle till to Mach 2.

Fig. 11 shows the angle of attack and the flap deflection needed to trim. If the CoG is in forward position, then the angle of attack that guarantees the vertical equilibrium in the experimental window at Mach 7.35 is -0.265 degrees; in this flight condition the static margin is higher than 5%. The flap deflection along the trajectory varies between -12 degrees and -17 degrees, with a manoeuvrability margin almost always bigger than 20% with a reduction to 15% only in the most demanding conditions when Mach is about 3.5, as already pointed out by the flyability analyses. If the CoG is in the rearward position, in the experimental window the angle of attack is -0.364 degrees and the static margin is slightly lower than 3%. The flap deflection to trim varies along the trajectory between -10.5 degrees and -15.7 degrees, with a manoeuvrability margin always bigger than 20%.

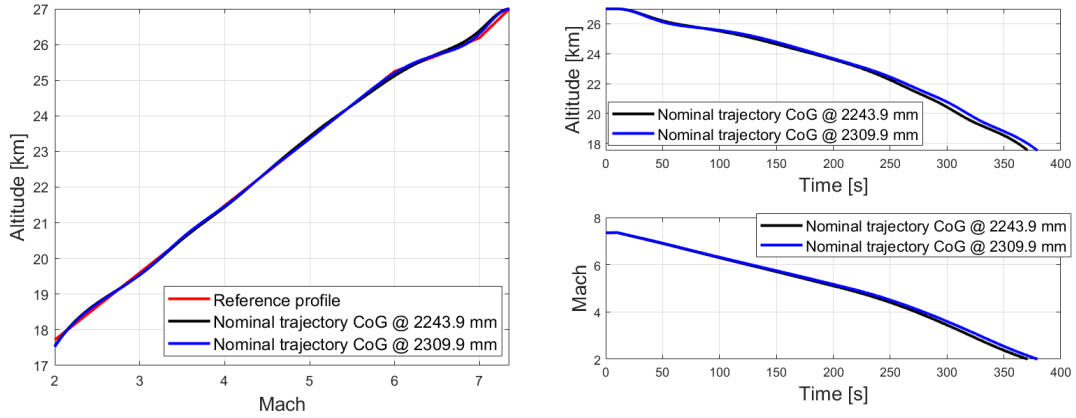

Fig 10. Nominal trajectories for different centre of gravity positions compared with the reference mission profile in the Mach-altitude plane (left) and plotted versus time (right)

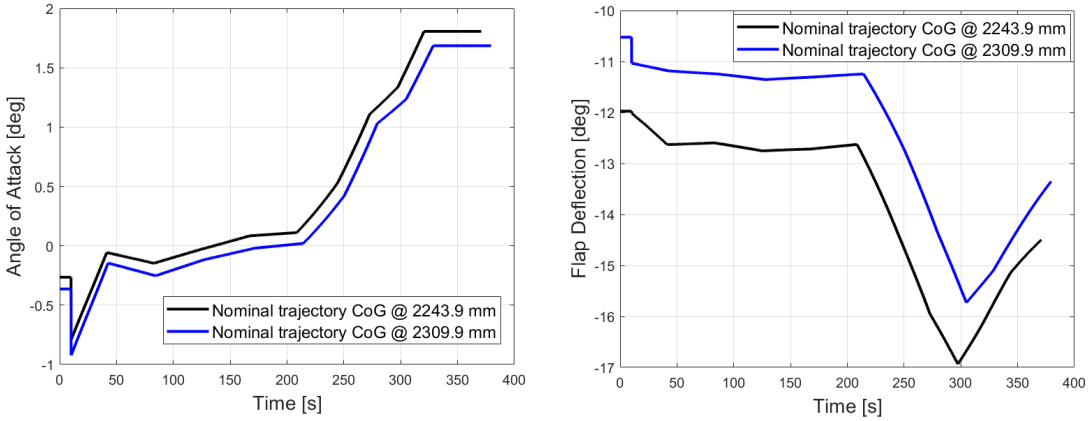

Fig 11. Time histories for different centre of gravity positions of the angle of attack (left) and flap deflection required to trim the vehicle along the nominal trajectory (right)

If the centre of gravity is rearward, then a smaller negative deflection of the flap is needed to trim the vehicle along the trajectory, coherently with Fig. 4. It produces a reduction of the drag and an increase of the lift with respect to the trajectory for forward CoG, as highlighted by Fig. 7, and therefore the angle of attack required to track the reference profile is slightly lower (few tenths of degrees) and the aerodynamic efficiency improves. The effects of the flap deflection are evident also on Mach and altitude; indeed, the vehicle with rearward centre of gravity decelerates and descends slower, increasing of few seconds the duration of the gliding phase. However, the differences between the two CoG positions are small, and in both cases the nominal trajectory is compliant with the preliminary thresholds defined at system level, which are shown in Fig. 12. The only exception is a pick for the heat flux at the end of the experimental window that very slightly exceeds the related threshold. This heat flux overshot is however considered within the system margins applicable in the current design phase of the project (the values of the system constraints are still preliminary), and anyway it can be mitigated simply reducing by few points percentage the velocity at the beginning of the experimental window.

In conclusion, both flyability analyses and nominal trajectory design confirm the feasibility of the mission.

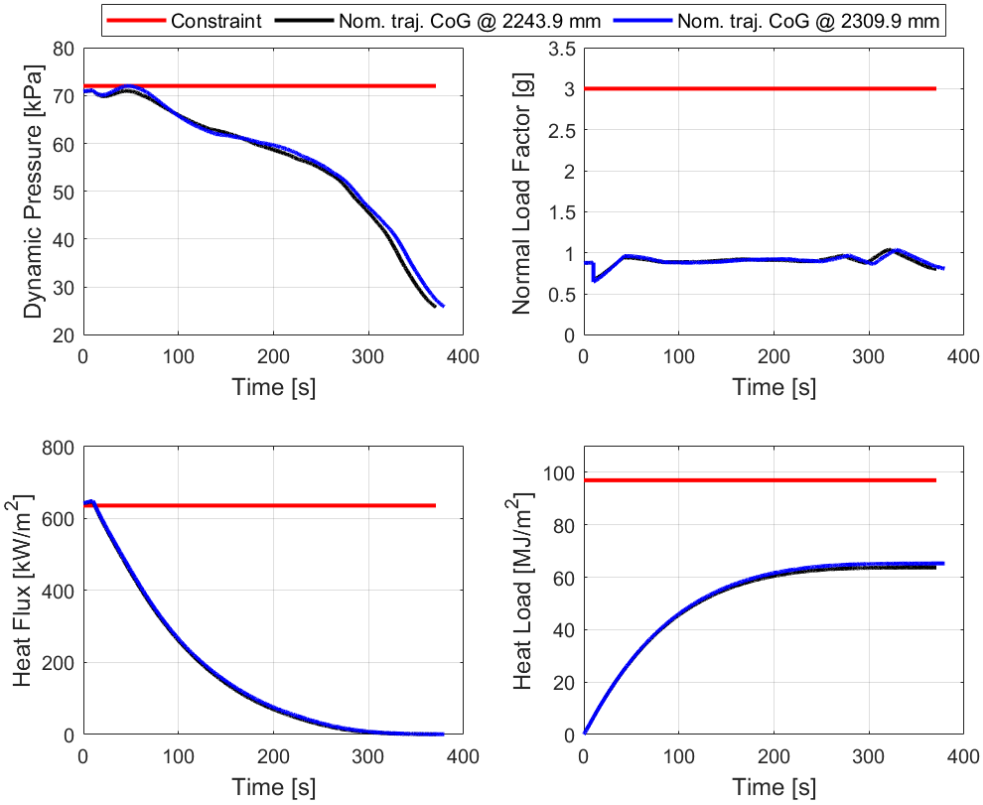

Fig 12. Computed trajectory's parameters for different centre of gravity positions versus preliminary allowable thresholds

5. Conclusions

This paper presented and discussed the flight mechanics analyses performed in the preliminary design phase of a hypersonic demonstrator, in order to assess the flyability properties of the vehicle and to define the nominal trajectory for the envisage mission concept.

The analyses allowed to identify the region in which the demonstrator's centre of gravity shall be located to have good flyability properties, which guarantee trimmability, manoeuvrability and static stability with margins typical of a hypersonic configuration. The identified centre of gravity allowable range along the vehicle longitudinal axis is only long 66 millimetres, requiring high accuracy and precision in locating the CoG, which shall be place slightly forward with respect to the initial selected nominal position.

The nominal trajectory was determined by solving a constrained nonlinear optimization problem. It has been presented for each of the two CoG positions that delimit the identified allowable range of variation for the centre of gravity. Both obtained trajectories are compliant with all the applicable mission requirements and preliminary system constraints.

In conclusion, the analyses provided useful information on the demonstrator configuration and confirmed the feasibility of the envisaged flight test.

Acknowledgements

The work has been co-funded by Italian Space Agency and CIRA ScPA in the frame of the agreement nr. 2022-13-HH.0-F43D22000410005.

References

1. Di Benedetto, S., Marini, M., Roncioni, P., Vitale, A., Vernillo, P., Cardone, S., Albano, M., Bertacin, R., Cavallini E.: Design of the Scramjet Hypersonic Experimental Vehicle. Aerospace

Europe Conference 2023 – 10TH EUCASS – 9TH CEAS (2023). https://doi.org/10.13009/EUCASS2023-899

2. Di Benedetto, S., Marini, M., Roncioni, P., Vitale, A., Vernillo, P., Cardone, S., Cavallini, E., Albano, M., Bertacin, R.: The Scramjet Hypersonic Experimental Vehicle. 3rd International Conference on High-Speed Vehicle Science Technology HiSST (2024)
3. Pezzella, G., Marini, M., Cicala, M., Vitale, A., Langener, T., Steelant, J.: Aerodynamic Characterization of HEXAFLY Scramjet Propelled Hypersonic Vehicle. 32nd AIAA Applied Aerodynamics Conference (2014). https://doi.org/10.2514/6.2014-2844
4. Morani, G., Corraro, F., Vitale, A.: New Algorithm for Probabilistic Robustness Analysis in Parameter Space. AIAA Journal of Aerospace Computing, Information, And Communication, Vol. 6, No. 4, 291-306 (2009). https://doi.org/10.2514/1.39338
5. Vitale, A., Corraro, F., Bernard, M., De Matteis, G.: Unscented Kalman Filtering for Reentry Vehicle Identification in the Transonic Regime. AIAA Journal of Aircraft, Vol. 46, No. 5, 1649-1659 (2009). https://doi.org/10.2514/1.42256
6. Vinh, N. X., Busemann, A., Culp, R. D.: Hypersonic and Planetary Entry Flight Mechanics. University of Michigan Press, Ann Arbor (1980)
7. Bahm, C., Baumann, E., Martin, J., Bose, D., Beck, R. E., Strovers, B.: The X-43A Hyper-X Mach 7 Flight 2 Guidance, Navigation and Control Overview and Flight Test Results. AIAA-2005-3275, AIAA/CIRA 13th International Space Planes and Hypersonics Systems and Technologies Conference (2005). https://doi.org/10.2514/6.2005-3275
8. Powell, M. J. D.: A Fast Algorithm for Nonlinearly Constrained Optimization Calculations. Numerical Analysis, ed. G. A. Watson, Lecture Notes in Mathematics, Springer-Verlag, Vol. 630 (1978)
9. Gill, P. E., Murray, W., Wright, M. H.: Practical Optimization. London, Academic Press (1981)